# Percolative phase separation induced by nonuniformly distributed excess oxygen in low-doped $La_{1-x}Ca_xMnO_{3+\delta}$ ($x \leqslant 0.2$)

Ilryong Kim, Joonghoe Dho, and Soonchil Lee
*Department of Physics, Korea Advanced Institute of Science and Technology, Taejon 305-701, Korea*
(Received 16 November 1999)

Zero-field $^{139}$La and $^{55}$Mn nuclear magnetic resonances were studied in $La_{0.8}Ca_{0.2}MnO_{3+\delta}$ with different oxygen stoichiometries $\delta$. The signal intensity, peak frequency, and line broadening of the $^{139}$La NMR spectrum show that excess oxygen atoms have a tendency to concentrate and establish local ferromagnetic ordering around themselves. These local orderings connect ferromagnetic clusters embedded in the antiferromagnetic host to form percolative ferromagnetic conduction paths. This phase separation is not a charge segregation type, but an electroneutral type. The magnetoresistance peak at the temperature where percolative paths start to form provides direct evidence that phase separation is one source of the colossal magnetoresistance effect.

## I. INTRODUCTION

Since the discovery of the colossal magnetoresistance (CMR) effect in $La_{1-x}Ca_xMnO_3$ (LCMO),[1] much theoretical and experimental work has been done to find the physical mechanism of the CMR effect because of its interesting physical properties and application potential. The explanation of the most interesting physical property of LCMO, the simultaneous occurrence of the paramagnetic to ferromagnetic and insulator to metal transitions, was the simple double-exchange model given by Zener in 1951.[2] However, Millis pointed out in 1995 that the resistivity of Sr-doped manganites cannot be fully explained by double-exchange alone.[3] Since then, several theories have been proposed to give a more complete description of the physical properties of CMR materials, one of which is phase separation (PS).

In the low doping range ($x \leqslant 0.2$), the magnetic phase of LCMO is not homogeneous. The existence of magnetic PS was verified by the simultaneous observation of ferromagnetic and antiferromagnetic nuclear magnetic resonance (NMR) signals at low temperature.[4] Since the ferromagnetic metallic regions embedded in the antiferromagnetic insulating host are not connected, LCMO is a ferromagnetic insulator for low Ca concentrations. Since then, PS has been suspected as one of the possible mechanisms of the CMR effect. On the other hand, PS has also been observed near the phase-transition temperature in LCMO for $0.2 < x < 0.5$, which are homogeneous ferromagnetic metals well below the transition temperature.[5,6] These two kinds of PS are thought to have originated from different mechanisms, because the PS observed in the low doping range is the ground state and stable in a wide temperature range, while the PS observed for $0.2 < x < 0.5$ occurs only near phase transition temperature. In this report, we will focus our discussion on the PS in low doped LCMO.

Theory predicts two different types of PS in low-doped LCMO. One is the charge segregation type and the other is the electroneutral type. Yunoki[7] studied the two-orbital Kondo model including the classical Jahn-Teller phonons and found that the PS is induced by the orbital degrees of freedom. Since in this case charge density of $e_g$ electrons is not stable at a special value of chemical potential, two regions with different charge densities are generated. The size of the regions is expected to be very small, about the order of a nanometer, due to the extended Coulomb interaction. Recently, Uehara presented TEM images of $La_{5/8-y}Pr_yCa_{3/8}MnO_3$,[8] which show the mixture of the charge ordering phase and ferromagnetic phase at low temperature. The size of both regions is about 0.5 $\mu$m, which is too large to be explained by the charge segregation type PS. On the other hand, Nagaev analyzed the PS induced by nonuniformly distributed oxygen.[9] He pointed out that the regions enriched with oxygen have an enhanced hole density and the holes establish local ferromagnetic ordering. In this case, PS is the electroneutal type because the densities of holes and excess oxygen are same in a given region, and the region size can be much larger than that of the charge segregation type PS. Several reports have supported the existence of PS, but it still remains unclear which scenario is more correct in low doped LCMO. There have been many works which showed that oxygen plays an important role in determining the electromagnetic properties of LCMO,[10,11] but its effects on PS have never been studied. In this work, we report that the electroneutral percolative PS is generated in low doped LCMO by excess oxygen. Our experimental results provide evidence that the PS in the low doping range is one source of the CMR effect.

## II. EXPERIMENT

Two polycrystalline samples of $La_{0.8}Ca_{0.2}MnO_{3+\delta}$ with different $\delta$ values were synthesized by the conventional solid-state reaction method. The starting materials were $La_2O_3$, $MnCO_3$, and $CaCO_3$. Calcining and sintering with intermediate grinding were repeated in the temperature range of 1000–1350 °C for four days. Sample 1 was obtained by annealing in air at 1100 °C for two days, and sample 2 was obtained by additional grinding, sintering, and annealing of a part of sample 1 in oxygen flow (200 cc/min) at the same temperatures as sample 1. The crystal structures were examined with a x-ray powder diffractometer using Cu $K\alpha$ radiation. Both samples had pure orthorhombic structure. The lattice parameters of sample 1 and 2 were $a_1 = 5.489$ Å, $b_1$

 

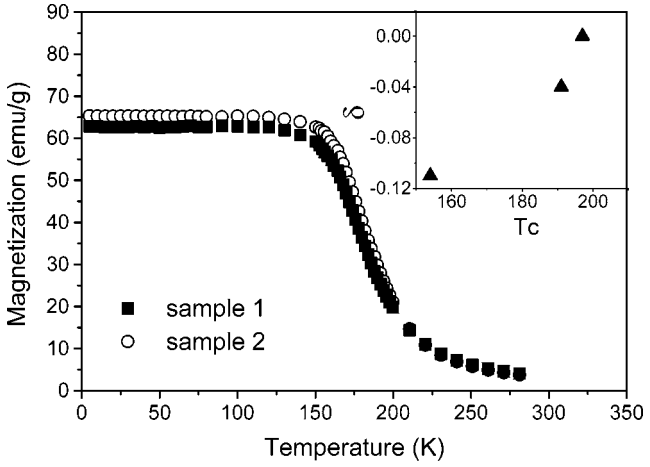


FIG. 1. The temperature dependence of magnetization at 1 T. Inset: $\delta$ vs $T_C$ (from Ref. 10).

$=5.496$ Å, $c_1=7.765$ Å, and $a_2=5.502$ Å, $b_2=5.507$ Å, $c_2=7.777$ Å, respectively. Resistivity was measured using the conventional four-probe method, and magnetization was measured by a commercial superconducting quantum interference device magnetometer. Zero-field NMR spectra were obtained by using the spin-echo technique. Since the spectra were very broad (about 4 MHz), echo heights were measured as a function of frequency after a partial spectral excitation. A 90°–180° pulse sequence was used for the echo generation and the width of the 90° pulse was 0.5 $\mu$s. The spin-echo time was fixed at 20 $\mu$s.

### III. RESULTS AND DISCUSSION

Figure 1 shows the temperature dependence of the magnetization obtained at 1 T. The paramagnetic Curie temperatures ($T_C$) of samples 1 and 2, which were determined by linear fits to the inverse susceptibilities in the paramagnetic region, were 194 and 196 K, respectively. Judging from the graph in the inset of Fig. 1 which shows $\delta$ vs $T_C$,[10] sample 2 has more oxygen than sample 1 and the difference in $\delta$ values is close to but not bigger than 0.02. The magnetizations of samples 1 and 2 were almost the same at low temperature, as is shown in the figure, and the magnetic-field dependences of the magnetizations were also almost the same.

Although the macroscopic magnetic properties of the two samples are quantitatively very similar, the local magnetic environments are quite different, as is seen in the $^{139}$La NMR spectra obtained at 78 K plotted in Fig. 2. In the figure, two differences are noticeable between the spectra of samples 1 and 2. First, the signal intensity of sample 2 is about five times that of sample 1, and second, the resonance frequency of sample 2 is higher and the linewidth is much broader on the high-frequency side, while the line shape of sample 1 is symmetric. The NMR line shapes of stoichiometric LCMO's have been reported to be a single Gaussian.[6,14] This means that sample 1 is stoichiometric and consequently, the $\delta$'s of samples 1 and 2 are about 0 and 0.02, respectively. We discuss the difference in signal intensity first.

The NMR signal intensity of a ferromagnet in zero field is proportional to $\eta V H_L/T$, where $\eta$ is the enhancement factor, V is the volume of the ferromagnetic region of a sample, and $H_L$ is the local field at the nuclei of interest. Since the magnetization, which is proportional to V, does not change, the change in the NMR signal intensity by extra oxygen is due to the change of the enhancement factor at a given temperature and frequency. In ferromagnetic NMR, generally both the signal and rf input is enhanced due to the accompanying oscillation of electronic magnetic moments. The NMR signal intensity vs rf power plotted in Fig. 3(a) provides experimental support for our claim. The figure shows that sample 2 gives its maximal signal at a much lower rf power than sample 1, meaning that the rf field is more enhanced in sample 2 than in sample 1. Since the enhancement factor is usually $10–10^2$ in domains and $10^2–10^4$ in domain walls,[12] this is interpreted as that sample 2 has domain walls while sample 1 does not.

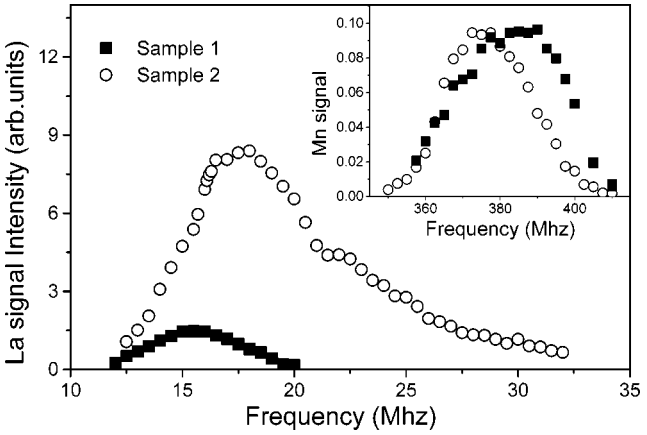


FIG. 2. The zero-field $^{139}$La NMR spectra obtained at 78 K. The frequency and the spin-spin relaxation time dependences of signal intensity were removed. Inset: the zero-field $^{55}$Mn NMR spectra obtained at 78 K. The intensity of sample 1 is amplified about 40 times.

Figure 3(b) provides direct evidence for this argument. The figure shows the normalized NMR signal intensity vs external magnetic field obtained at the fixed rf power which makes the maximal signal in zero field. In this figure, we notice that the signal of sample 2 decays almost to zero, while that of sample 1 decays slowly, approaching the saturation field at about 3 kOe. These are the typical responses of

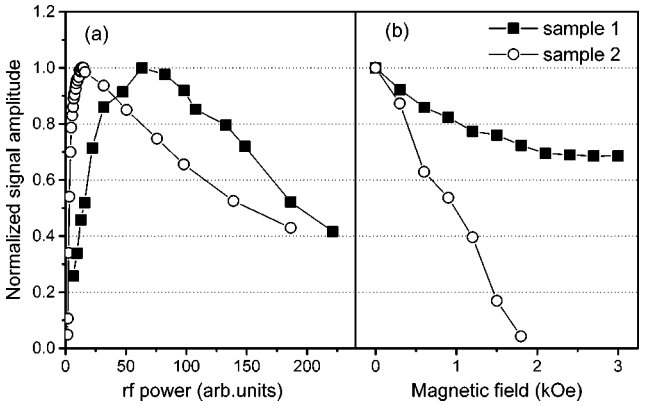


FIG. 3. The rf-power dependence (a), and external magnetic-field dependence (b), of the $^{139}$La NMR signal intensity obtained at 78 K.

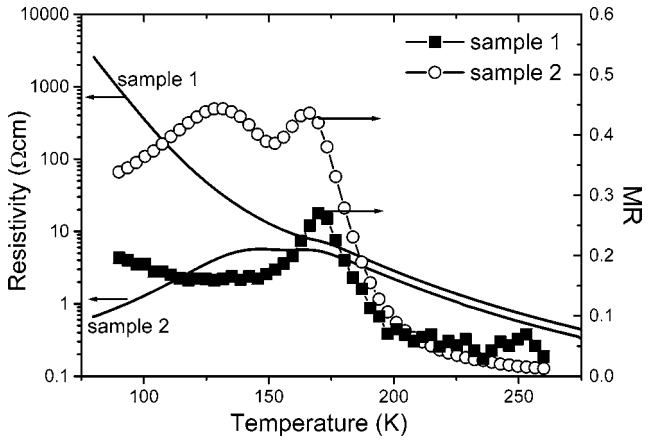


FIG. 4. The temperature dependence of the resistivity and magnetoresistance (MR). The MR value is defined as $[\rho(0) - \rho(9\ \text{kOe})]/\rho(0)$.

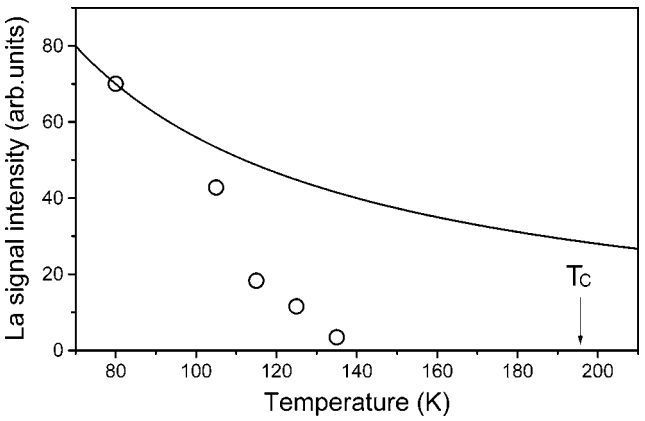


FIG. 5. The temperature dependence of the $^{139}$La NMR intensity of sample 2. The signal dependence on the spin-spin relaxation time and frequency were carefully eliminated from the raw data. The solid line represents a $T^{-1}$ curve.

single and multidomain ferromagnets, respectively. Since the domain walls disappear approaching the saturation field, the signal intensity of multidomain ferromagnets decays quickly. The signal of sample 1 decays a little because the enhancement factor decreases with external field, whereas the drastic signal decay of sample 2 indicates the disappearance of the domain walls. The NMR signal of sample 2 comes mostly from domain walls because the enhancement factor is usually orders of magnitude larger in domain walls than in domains. The size of ferromagnetic clusters embedded in the antiferromagnetic host of sample 1 is not large enough to form a multidomain state. The local ferromagnetic orderings generated by excess oxygen connect some of these ferromagnetic clusters and domain walls are formed on them.

In fact, these connected ferromagnetic clusters also make percolative conduction paths as is shown in Fig. 4 which displays the temperature dependence of the resistivity. The resistivity of sample 1 shows an insulating behavior, while that of sample 2 shows a broad peak in the temperature range of 170–140 K and metallic behavior below 140 K. The metallic behavior of sample 2 at low temperature implies that electric transport paths are formed by excess oxygen.

The temperature dependence of the La NMR signal intensity of sample 2 shown in Fig. 5 proves the simultaneous generation of conduction paths and domain walls. The signal intensity of homogeneous ferromagnets such as LCMO for $0.2<x<0.5$ follow Curie's $T^{-1}$ law well except in the narrow region near $T_C$.[6] However, the signal intensity of sample 2 decreases much faster than $T^{-1}$ with increasing temperature, and almost disappears near 140 K where the metallic behavior fades out (Fig. 4). This means that the total volume of domain walls decreases as the temperature increases and the ferromagnetic and metallic conduction paths vanish near 140 K. Approaching this temperature from below, ferromagnetic clusters are disconnected and therefore conduction paths are broken continuously.

While the magnetoresistance (MR) curve of stoichiometric perovskite manganite crystals show only one peak near $T_C$, that of sample 2 shows another peak near 140 K as is seen in Fig. 4. The MR peak near 170 K is an ordinary CMR peak due to the suppression of spin fluctuation by the external field, while the peak near 140 K is undoubtedly related to PS. It is worthwhile to note that the MR near the temperature where the percolative PS is induced is as large as that near the phase-transition temperature. It is believed that the external field makes hole transportation easier by suppressing spin fluctuation in the regions connecting metallic clusters.

We now discuss the second difference between the spectra of samples 1 and 2, the difference in resonance frequency and linewidth. The local field $H_L$ at the position of a nonmagnetic $La^{3+}$ ion can be described as

$$H_L = A\sum_j n_j\mu_j + H_{d-d},$$

where $A$ is the transferred hyperfine coupling constant and $n_j$ is the number of the $j$-site Mn moments $\mu_j$, surrounding the La ion. $H_{d-d}$ is the dipolar field summed over all Mn magnetic moments. In perovskite manganites, the dipolar field is negligible and the main contribution to $H_L$ comes from the transferred hyperfine field. The transferred hyperfine field is thought to be produced by the $\pi$ type overlapping between the Mn $t_{2g}$ electron wave function and the oxygen $|2p_\pi\rangle$ wave function, and the $\sigma$ bonding of the oxygen with the $|sp^3\rangle$ hybrid states of the $La^{3+}$ ion.[13] That is, an indirect transferred hyperfine field of the Fermi contact type is mediated by oxygen. Therefore, the constant $A$ is a function of the distance between oxygen and a $La^{3+}$ ion, and the number of oxygen atoms surrounding the $La^{3+}$ ion. $n_j$ and $\mu_j$ are almost the same in the two samples. The distance between oxygen and a $La^{3+}$ ion is not an important factor in the difference between the NMR peak frequencies because the peak frequency of sample 2 is higher than that of sample 1 even though the lattice constants of sample 2 are slightly larger than those of sample 1.[14] Therefore, the difference in peak frequency should be attributed to the difference in the number of oxygen atoms surrounding a $La^{3+}$ ion. That is to say, the peak frequency of sample 2 is increased due to the excess interstitial oxygen. There is a report that $LaMnO_{3+\delta}$ with excess oxygen is characterized by cation vacancy in La and Mn sites rather than by interstitial anions.[15] In this case, however, the lattice parameters decrease as $\delta$ increases contrary to our case.[16] Moreover, the NMR spectrum of

$LaMnO_{3+\delta}$ having cation vacancy is well fitted by a single Gaussian curve, while our sample 2 is not, as is discussed below.

The La NMR spectrum of sample 2 is asymmetric and broader than that of sample 1 on the high-frequency side. Since $\delta$ is small, homogeneous distribution of oxygen cannot enhance the signal in the high-frequency side as much as the spectrum in Fig. 2. Therefore, oxygen atoms aggregate to make local ferromagnetic orderings consistent with Nagaev's claim that oxygen has a tendency to concentrate. One of the reasons why conduction paths are continuously disconnected approaching 140 K could be the distribution of excess oxygen becoming more and more uniform as the temperature increases.

Contrary to La nuclei, the local field at Mn nuclei is negligibly influenced by the local distribution of oxygen because the hyperfine field of the direct Fermi contact type generated by its own $3d$ electrons is much stronger. Therefore, the Gaussian shape of the Mn NMR spectrum is not changed by the presence of excess oxygen as is shown in the inset of Fig. 2. The $^{55}$Mn NMR spectra are motionally narrowed by the fast hopping of $e_g$ electrons between $Mn^{3+}$ and $Mn^{4+}$ ion sites.[17,18] Only the Mn nuclei in ferromagnetic regions with the delocalized $e_g$ electrons contribute to the $^{55}$Mn NMR signal. The local field at Mn nuclei is proportional to the average number of delocalized $e_g$ electrons. The peak frequency shift due to excess oxygen is greater than or equal to 10 MHz. If the distribution of holes is uniform, such a shift corresponds to $\delta \sim 0.075$,[18] while the $\delta$ of sample 2 is less than 0.02. This means that the holes are concentrated in ferromagnetic regions. The results of La and Mn NMR imply that the oxygen and holes are concentrated in ferromagnetic regions. This supports the idea that the PS in low doped LCMO is of the electroneutal type. Moreover, considering the easy formation of conduction paths by the aggregation of excess oxygen whose concentration is less than 0.7%, the size of ferromagnetic clusters is not as small as predicted by the charge segregation type PS.

In conclusion, the excess oxygen atoms have a tendency to aggregate and change their surroundings into the ferromagnetic phase. These local ferromagnetic regions connect ferromagnetic clusters in stoichiometric samples, which are suspected to also be generated by inhomogeneous distribution of oxygen. This connection produces percolative conduction paths on which domain walls are formed. The observed PS is an electroneutral type rather than a charge segregation type. As the temperature increases, a MR peak was observed at the temperature where the percolative PS disappears, in addition to the ordinary peak near the phase-transition temperature.

## ACKNOWLEDGMENTS

We would like to thank Professor Ewan Stewart for his careful reading of this manuscript and suggesting improvements and corrections.

[1] S. Jin *et al.*, Science **264**, 413 (1994).
[2] C. Zener, Phys. Rev. **82**, 403 (1951).
[3] A.J. Millis *et al.*, Phys. Rev. Lett. **74**, 5144 (1995).
[4] G. Allodi *et al.*, Phys. Rev. B **56**, 6036 (1997).
[5] M.K. Gubkin *et al.*, Pis'ma Zh. Eksp. Teor. Fiz. **60**, 57 (1994) [JETP Lett. **60**, 57 (1994)].
[6] Joonghoe Dho *et al.*, Phys. Rev. B **59**, 492 (1999).
[7] S. Yunoki *et al.*, Phys. Rev. Lett. **81**, 5612 (1998).
[8] M. Uehara *et al.*, Nature (London) **399**, 560 (1999).
[9] E.L. Nagaev, Phys. Lett. **218**, 367 (1996).
[10] S. Tamura, Phys. Lett. **78A**, 401 (1980).
[11] H.L. Ju *et al.*, Phys. Rev. B **51**, 6143 (1995).
[12] E. A. Turov *et al.*, *Nuclear Magnetic Resonance in Ferro- and Antiferromagnets* (Halsted, New York, 1972).
[13] G. Papavassiliou *et al.*, Phys. Rev. B **55**, 15 000 (1997).
[14] G. Papavassiliou *et al.*, Phys. Rev. B **59**, 6390 (1999).
[15] B.C. Tofield *et al.*, J. Solid State Chem. **10**, 183 (1974); J.H. Kuo *et al.*, *ibid.* **83**, 52 (1989).
[16] R. Mahendiran *et al.*, Phys. Rev. B **53**, 3348 (1996); J. Töpfer and J.B. Goodenough, J. Solid State Chem. **130**, 117 (1997); A.M. De Léon-Guevara *et al.*, Phys. Rev. B **56**, 6031 (1997).
[17] Gen Matsumoto, J. Phys. Soc. Jpn. **29**, 615 (1970).
[18] Joonghoe Dho *et al.*, Phys. Rev. B **60**, 14 545 (1999).